Advances in Energy Science and Technology
Vol. 1, No. 4| Apr 2025
AEST

Crack evolution on plasma-facing materials under the heat loads of tokamaks

Ali Masoudi [a], **Davoud Iraji** [a,*], **Chapar Rasouli** [b]

[a] *Department of Physics and Energy Engineering, Amirkabir University of Technology, Hafez Ave, Valiasr Square, Tehran, 1591634311, Iran*

[b] *Plasma Physics and Nuclear Fusion Research School, Nuclear Science and Technology Research Institute, North Kargar Ave, Tehran, 14155-1339, Iran*

Keywords

Plasma-facing materials
Tokamak
Thermal loads
Plasma
Crack

Article Info

DOI:10.22060/aest.2026.25423.1003

Received date: 10 January 2026

Accepted date 1 April 2026

Published date 1 April 2026

* **Corresponding author:**
Iraji@aut.ac.ir

Abstract

Crack formation in plasma-facing materials (PFMs) under extreme transient heat loads poses a critical challenge for tokamak operation. This study investigates crack initiation and propagation in tungsten PFMs subjected to high transient heat fluxes using finite element simulations based on the Johnson–Cook constitutive model. Simulations were conducted for heat loads of 100 MJ/m² and 60 MJ/m² to capture the effects of both load amplitude and exposure time. At 100 MJ/m², cracks initiated at 0.15 s from the sample edges and propagated symmetrically toward the center, eventually leading to surface delamination. For 60 MJ/m², crack initiation was delayed to 0.5 s, with slower propagation and less extensive damage, demonstrating the strong dependence of crack evolution on both thermal load and duration. The analysis revealed that Mode I (opening mode) cracking predominates, driven by load gradients between surface and subsurface elements. These results provide quantitative insight into the thresholds for structural instability in tungsten PFMs and highlight the critical role of transient thermal stresses in predicting material performance under tokamak conditions. The findings offer valuable guidance for the design, selection, and engineering of PFMs in future fusion reactors.

Graphical Abstract

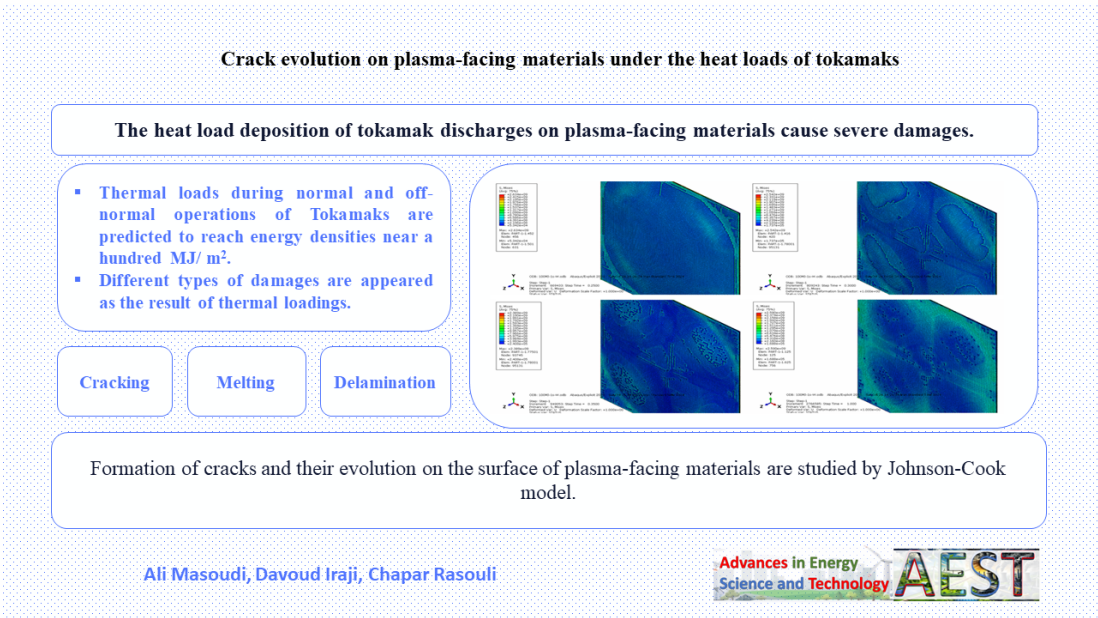

Advances in Energy Science and Technology
Vol. 1, No. 4| Apr 2025
AEST

1. Introduction

Plasma-facing materials (PFMs) in magnetic confinement fusion devices are required to withstand extreme thermal environments arising from both steady-state and transient energy deposition on plasma-exposed surfaces [1]. In steady operation, PFMs must continuously absorb heat fluxes on the order of ~10- 20 $MW\,m^{-2}$, but short, intense thermal pulses associated with plasma instabilities present additional and often greater challenges. These transient loads include repetitive edge-localized modes (ELMs) that accompany high-confinement (H-mode) operation and deposit bursts of energy over milisecond and sub-millisecond durations with heat fluxes approaching the $GW\,m^{-2}$ range, imposing repeated thermal shock on divertor targets and first-wall surfaces [2–6].

Beyond such operational transients, off-normal events—including plasma disruptions, vertical displacement events (VDEs), and intense impacts from runaway electrons (REs)—can deliver significantly higher energy densities over very short timescales, reaching hundreds of $MW\,m^{-2}$ to tens of $GW\,m^{-2}$ and producing severe thermal shock and stress fields in PFMs [7–12].

Among candidate PFMs, tungsten has emerged as the primary divertor and first-wall material for ITER and future reactors due to its high melting point (~3422 °C), low sputtering yield, relatively low tritium retention, and strong thermal conductivity. Despite these advantageous properties, tungsten exhibits brittle behavior at lower temperatures and undergoes thermal fatigue cracking when subjected to repeated transient heat loads, especially below its ductile-to-brittle transition temperature (DBTT) [13,14].

High-heat-flux experiments and plasma device exposures have consistently shown that ELM-like pulses cause surface roughening, localized melting, recrystallization, and the initiation of crack networks on tungsten surfaces. The morphology and depth of these cracks are sensitive to both the heat flux intensity and the transient duration, with deeper and more extensive cracking occurring at higher flux levels and increased pulse repetition [15–17].

During off-normal transient events such as disruptions and VDEs, the damage can be more severe, including extensive melting and surface degradation, which can also contribute to impurity release into the core plasma [18]. Understanding and predicting how tungsten and tungsten-based materials respond to these thermal shocks is essential for designing robust PFMs [19]. Numerical modeling, especially finite element analysis (FEA), plays a central role in interpreting experiments and extrapolating behavior toward reactor-relevant conditions where direct experimental replication is impractical. However, accurate simulation of transient heat load effects requires constitutive models that can represent thermo-mechanical behavior under rapid heating and cooling, including plastic deformation, strain-rate effects, and thermal softening.

The aim of this work is to study the formation of cracks on the PFMs due to tokamak thermal loads and investigate how the crack are propagated by increasing the energy and the heat load durations. The paper is organized as follows: Section 2, describes theoretical basis about tokamak heat loads, their effects and the damage model. Simulation of the transient thermal loads on the PFMs is demonsterated and discussed in Section 3. Finally, the research conclusion is presented in Section 4.

2. Theoretical basis

2.1. Transient Heat Load Effects on Plasma-Facing Materials

Transient heat loads deposited on the PFM surfaces generate highly non-uniform temperature fields characterized by steep gradients normal to the exposed surface. Owing to the short duration of ELM-like and disruption-like events, the thermal

diffusion length remains limited to the near-surface region, resulting in localized heating followed by rapid cooling once the heat pulse terminates. The steep temperature gradients of the surface, leads to significant thermal stresses [20]. PFMs must accommodate these gradients with minimal structural degradation. The magnitude of thermo-mechanical loading depends on the peak heat flux, pulse duration, the base temperature of the material and its thermal physical properties such as conductivity and expansion coefficient [8].

Actually, the constrained thermal expansion of the heated layer against colder underlying material generates high thermal stresses, which can exceed the yield strength of the PFM and initiate plastic deformation. Upon cooling, tensile stresses develop as the constrained material contracts, promoting the nucleation and growth of cracks. The detailed process of crack formation depends on the local microstructure, base temperature relative to DBTT, and the heat flux parameters. Transient heat loads are therefore capable of inducing both micro-scale damage such as dislocation movements and larger network cracks visible by microscopy.

Under repeated transient loading, surface crack networks emerge as a dominant damage mode, as cyclic thermal stresses cause near-surface zones to yield plastically and then fracture upon cooling [21,22].

Experiments using hydrogen plasma exposures followed by pulsed heating tests have demonstrated that preloading with plasma increases crack density and affects crack morphology, indicating a synergy between plasma exposure and thermal shock behavior [23,24].

These observations align with studies of combined transient and steady exposure showing reduced damage thresholds under simultaneous loads due to elevated defect density and embrittlement effects [25].

2.2. Johnson–Cook Constitutive Model

To capture the complex plastic response of the PFMs under these rapid thermal transients, a constitutive model that includes strain hardening, strain-rate sensitivity, and thermal softening is needed. The Johnson–Cook (JC) model is a phenomenological constitutive formulation originally developed to describe the flow stress of metals across wide ranges of temperature and strain rate. In this model, the equivalent flow stress σ is expressed as:

$$\sigma=[A+B(\varepsilon)^{n}]\left[1+C\ln\left(\frac{\dot{\varepsilon}}{\dot{\varepsilon}_0}\right)\right]\left[1-\left(\frac{T-T_{ref}}{T_{melt}-T_{ref}}\right)^{m}\right] \quad (1)$$

where ε is equivalent plastic strain, $\dot{\varepsilon}$ is strain rate, *A, B, C, n, m* are calibrated material constants, and *T* is temperature relative to a reference temperature T_{ref} and melting temperature T_{melt} [26–28].

In commercial finite element software like Abaqus, the Johnson–Cook plasticity model (and associated damage models) can be used for coupled thermo-mechanical analysis. Transient heat loads applied as time-dependent surface heat flux boundary conditions generate temperature fields, which are coupled to mechanical fields through thermal expansion and temperature-dependent material properties. The plastic response governed by a JC model allows prediction of stress and plastic strain distribution during heating and cooling cycles, providing insight into likely locations of crack initiation and growth.

In the standard JC implementations, localized zones of accumulated plastic strain and high tensile stress serve as proxies for damage and indicate where cracks are most likely to initiate under repeated transient loading [29].

The purpose of this study is to simulate the crack formation on the surface of the PFM. **Fig. 1** presents the block diagram of the simulation process.

Advances in Energy Science and Technology
Vol. 1, No. 4| Apr 2025
AEST

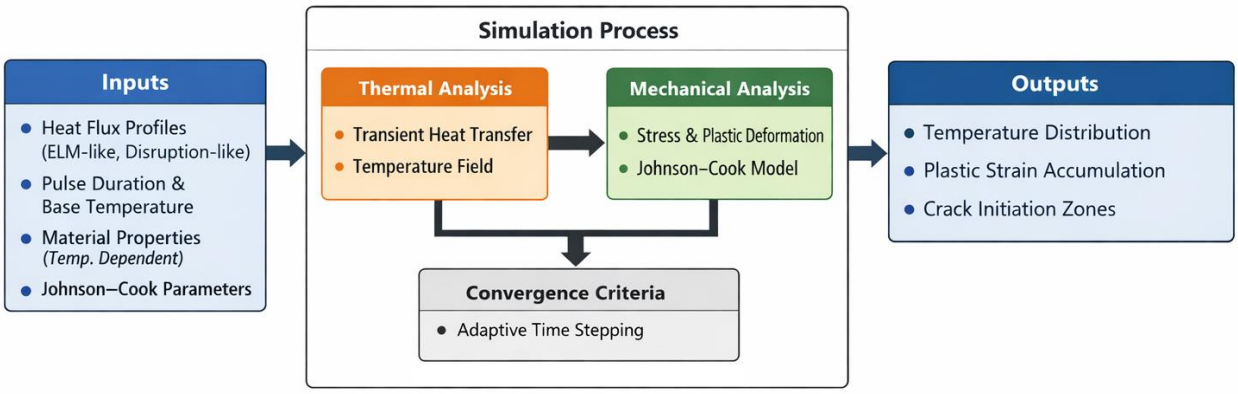

Fig. 1. Simulation workflow of PFM under transient heat loads.

3. Results and discussion

This study presents the simulation results of applying thermal loads on tungsten samples through the JC constitutive model. The criteria over which the fracture of the material occurs is the Von Mises Stress of the order of GPa on the sample surface. For the simulations, the JC constitutive model parameters for tungsten plasma-facing materials were adopted from the literature (Refs. [30–32]).

The modeled sample is a homogeneous cuboid tungsten with dimensions of 1×1×0.01 m^3, subjected to a uniform heat load applied to the front surface. A fixed temperature of 50 °C is imposed as a boundary condition on the bottom surface. The remaining surfaces are constrained against both displacement and rotation. The total simulation time is 1 *s*, and the model consists of 78,125 finite elements.

In the simulations, heat loads exceeding typical tokamak transient levels were applied to the sample, with a simulation duration of 1 *s* to represent a condition in which all tokamak heat loads act simultaneously on the PFM. Using this approach, the strength of the tungsten PFM and the stress levels leading to crack initiation were evaluated. Accordingly, a heat load of 100 *MJ* was first applied for 1 *s* (the energy density of 100 MJ/m^2). The heat load was then reduced to 60 *MJ*, while the simulation time was extended to 2 *s*, to compare the relative effects of heat-load magnitude and application time.

Fig. 2 and **Fig. 3** illustrate the stress distribution at different time steps for an applied heat load of 100 *MJ*. **Fig. 2a–2d** present the simulation results at time steps of 0.05 *s*, 0.1 *s*, 0.15 *s*, and 0.2 *s*, respectively. As shown in **Fig. 2 (a)**, at 0.05 *s* the maximum von Mises stress reaches 1.48 *GPa*, while the minimum stress is 2.23 *kPa*. At this stage, the maximum stress is concentrated at the surface corners. This stress localization is attributed to the applied boundary conditions, which restrict displacement at the corners and consequently lead to stress amplification in these regions.

At 0.1 *s*, the maximum and minimum stresses increase to 1.91 *GPa* and 3.95 *kPa*, respectively, and the stress distribution becomes nearly uniform across the surface (**Fig. 2b**). After 0.15 s, the maximum stress rises to 2.44 *GPa* and the minimum stress to 10 *kPa*. As shown in **Fig. 2c**, at this time step, the surface stress remains uniformly distributed; however, element distortion begins to appear at the edges, indicating the onset of crack initiation.

When the time step reaches 0.2 *s* (**Fig. 2d**), the stress distribution remains uniform over the surface, while the number of damaged elements at the edges increases. The corresponding maximum and minimum stresses reach 2.58 *GPa* and 33.5 *kPa*, respectively. Overall, it can be concluded that both the maximum and minimum von Mises stresses increase progressively as the simulation time advances from 0.05 s to 0.2 *s*.

Advances in Energy Science and Technology
Vol. 1, No. 4| Apr 2025
AEST

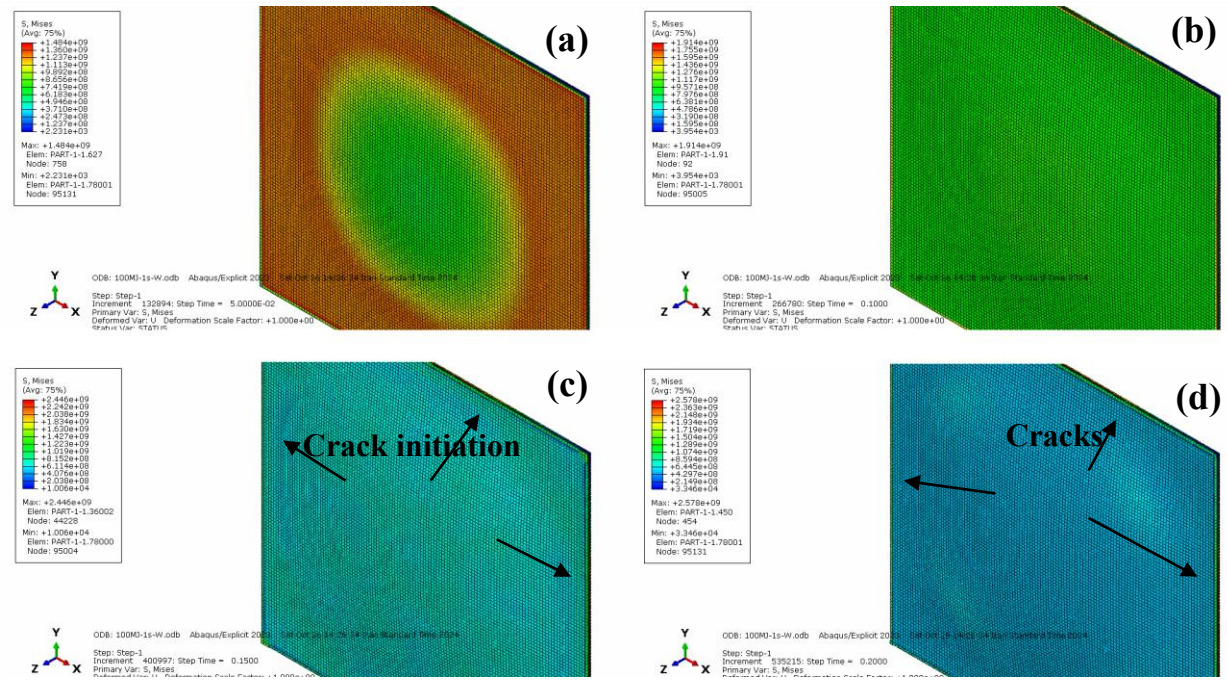

Fig. 2. Von Mises stress distribution on the tungsten sample under a uniform heat load of 100 *MJ* at different time steps: (a) 0.05 *s*, (b) 0.1 s, (c) crack initiation at the edges at 0.15 *s*, and (d) crack propagation at 0.2 *s*.

Fig. 3a–3d illustrates the progressive growth of cracks from the sample edge toward the center of the surface at step times of 0.25 *s*, 0.3 *s*, 0.35 *s*, and 1 *s* under a heat load of 100 *MJ*. The results show that the surface damage expands symmetrically from the edges, eventually leading to the disappearance of most surface elements and the onset of delamination.

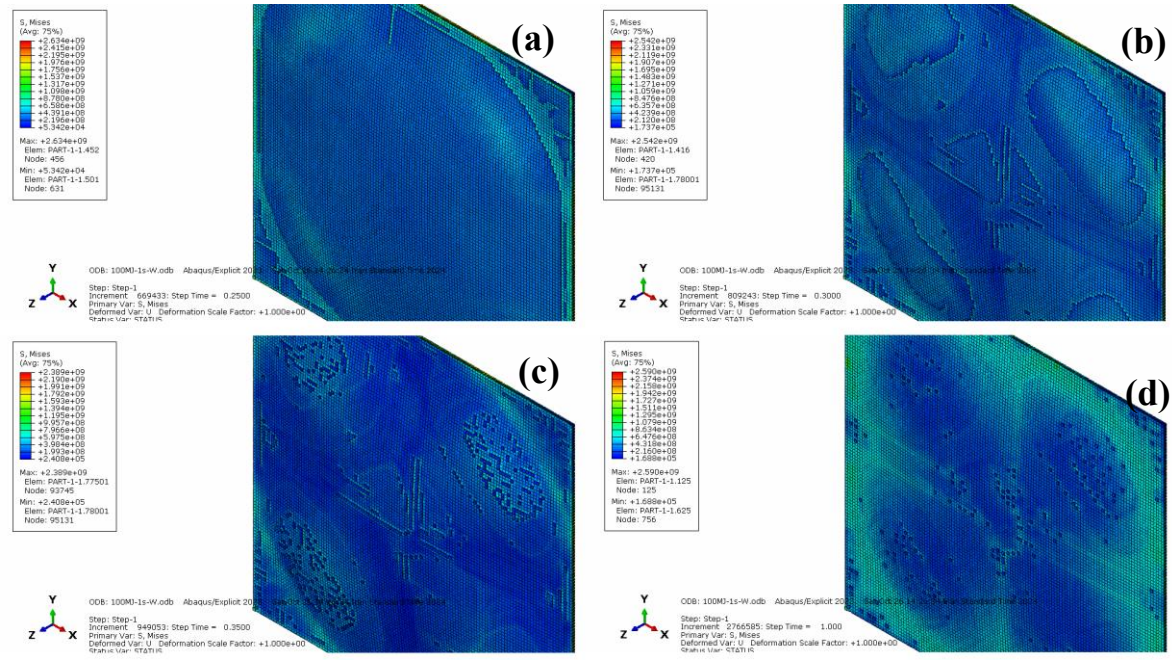

Fig. 3. Simulation of crack propagation on the tungsten sample under a 100 MJ heat load; (a) t =0.25 *s*, (b) t =0.3 *s*, (c) t =0.35 *s*, (d) t =1 *s*, showing the symmetric growth of cracks from the sample edge toward the center and the eventual surface delamination.

Advances in Energy Science and Technology
Vol. 1, No. 4| Apr 2025
AEST

Fig. 4 and **Fig. 5** illustrate the stress distribution for a heat load of 60 *MJ* over a simulation time of 2 *s*. As shown in **Fig. 4a-4b**, at this load, the stress pattern resembles that observed for 100 *MJ*. **Fig. 4c** shows that cracks initiate at the sample edges at a step time of 0.5 *s*, where the maximum stress is 2.57 *GPa* and the minimum stress is 23.3 *kPa*. By 0.7 *s*, the cracks have propagated toward the center, as seen in **Fig. 4d**. Notably, both the maximum and minimum stresses at crack initiation are higher than those for the 100 *MJ* load, which is consistent with the longer initiation time compared to that case.

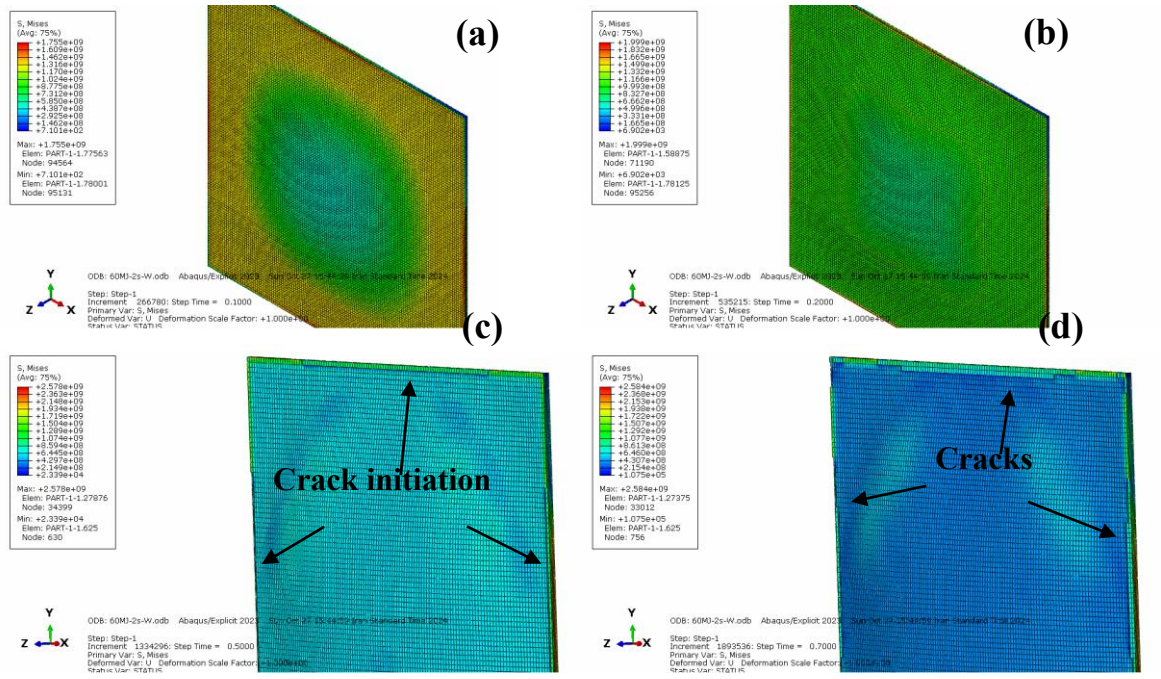

Fig. 4. Von Mises stress distribution on the tungsten sample under a uniform heat load of 60 MJ at different time steps: (a) 0.1 *s*, (b) 0.2 *s*, (c) crack initiation at the edges at 0.5 *s*, and (d) crack propagation at 0.7 *s*.

By extending the duration of the applied heat load, **Fig. 5a-5d** illustrates the evolution of cracks at step times of 1 *s*, 1.3 *s*, 1.6 *s*, and 2 *s*, respectively. From these images, it is evident that the crack pattern maintains a symmetric distribution, similar to that observed at a heat load of 100 *MJ*. It is also apparent that reducing the heat load delays the onset of damage, with cracks appearing at later step times.

Advances in Energy Science and Technology
Vol. 1, No. 4| Apr 2025
AEST

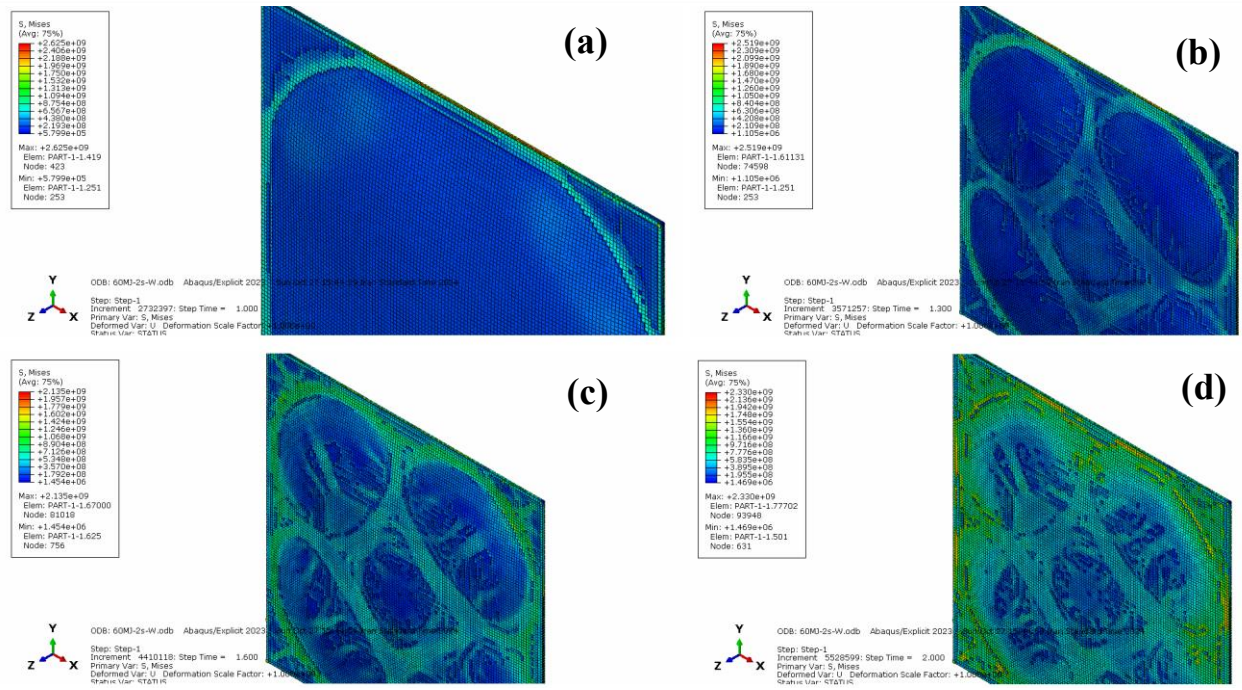

Fig. 5. Simulation of crack propagation on the tungsten sample under a 60 MJ heat load; (a) t = 1 s, (b) t = 1.3 s, (c) t = 1.6 s, (d) t = 2 s, showing the symmetric growth of cracks from the sample edge toward the center and the eventual surface delamination.

Crack propagation occurs in three modes: Mode I, or opening mode, where tensile stress acts perpendicular to the crack plane; Mode II, or sliding mode, where shear stress acts parallel to the crack plane and perpendicular to the crack front; and Mode III, or tearing mode, where shear stress is parallel to both the crack plane and the crack front [33]. Although the surface heat load is applied uniformly, the surface elements experience different loads compared to the underlying elements. The 0.01 *m* thick sample was divided into five layers for meshing, and this load difference between surface and back-layer elements can induce cracking. The simulation results indicate that Mode I crack propagation occurs primarily between the surface elements and those in the back layer.

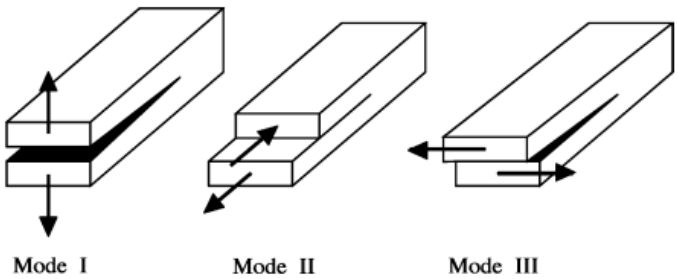

Fig. 6. Three fundamental crack propagation modes: Mode I (opening), Mode II (sliding), and Mode III (tearing).

4. Conclusion

This study investigated the evolution of cracks on plasma-facing materials under transient heat loads representative of tokamak conditions, using computational approaches. Finite element simulations of tungsten samples, employing the Johnson–Cook constitutive model, revealed the initiation and growth of cracks under heat loads of 100 MJ/m^2 and 60 MJ/m^2. At 100 MJ/m^2, crack initiation occurred at 0.15 *s*, followed by rapid propagation from the edges toward the center, with

symmetric damage patterns and eventual surface delamination. For 60 MJ/m^2, crack initiation was delayed to 0.5 s, and propagation occurred more gradually, demonstrating the strong dependence of damage onset and growth on both heat load amplitude and exposure time.

The simulations also highlighted that cracks primarily propagated in Mode I (opening mode) between surface and subsurface elements, consistent with the load gradients across layers. The results provide critical insight into the thresholds for structural instability of tungsten PFMs under extreme transient heat fluxes and establish a quantitative basis for predicting crack formation and growth in tokamak-relevant conditions. These findings emphasize the importance of considering both heat load magnitude and duration in the design and evaluation of plasma-facing components for future fusion reactors.

Author contributions

A. M. conceived the idea, conceptualized the research, performed the computer simulations, and wrote the paper. **D. I.** supervised the project, directed the research, and revised the manuscript. **C. R.** validated, Investigated, administrated the project, reviewed and edited the manuscript.

Declaration of competing interest

The authors declare that they have no known competing financial interests or personal relationships that could have appeared to influence the work reported in this paper.

Data availability

Data will be made available on request.

References

[1] A. Masoudi and D. Iraji, Investigation of glow discharge plasma energy distribution using a gridded energy analyzer considering plasma-facing materials related processes, Fusion Eng. Des. 212, (2025) 114862.

[2] M. Gago, S. Antusch, A. Klein, A. Kreter, C. Linsmeier, M. Rieth, B. Unterberg, and M. Wirtz, Thermal Shock and Synergistic Plasma and Heat Load Testing of Powder Injection Molding Tungsten-Based Alloys, J. Nucl. Eng. 6, (2025).

[3] R. A. Pitts, S. Carpentier, F. Escourbiac, T. Hirai, V. Komarov, S. Lisgo, A.S. Kukushkin, A. Loarte, M. Merola, A.S. Naik, R. Mitteau, A full tungsten divertor for ITER: Physics issues and design status, J. Nucl. Mater. 438, (2013) 48.

[4] G. Federici, C.H. Skinner, J.N. Brooks, J.P. Coad, C. Grisolia, A.A. Haasz, A. Hassanein, V. Philipps, C.S. Pitcher, J. Roth, W.R. Wampler, Plasma-material interactions in current tokamaks and their implications for next step fusion reactors, Nucl. Fusion 41, (2001) 1967-2137.

[5] V. Sizyuk and A. Hassanein, New proposed ITER divertor design using carbon insert on tungsten to mitigate ELMs and secondary radiation effects on nearby components, Sci. Rep. 12, (2022) 4698.

[6] J. Linke, J. Du, T. Loewenhoff, G. Pintsuk, B. Spilker, I. Steudel, and M. Wirtz, Challenges for plasma-facing components in nuclear fusion, Matter Radiat. Extremes 4, (2019) 056201.

[7] A. Masoudi, D. Iraji, and C. Rasouli, Investigation of the effects of transient heat loads on plasma-facing materials in Tokamaks, Adv. Energy Sci. Technol. 1, (2025) 1.

[8] A. Masoudi, D. Iraji, and C. Rasouli, Edge-localized-mode heat load effects on plasma-facing materials studied using runaway electrons in the Damavand tokamak, Phys. Rev. E 112, (2025) 45217.

[9] A. Hassanein, T. Sizyuk, V. Sizyuk, and G. Miloshevsky, Impact of various plasma instabilities on reliability and performance of tokamak fusion devices, Fusion Eng. Des. 85, (2010) 1331.

[10] A. Fedrigucci, N. Marzari, and P. Ricci, Comprehensive Screening of Plasma-Facing Materials for Nuclear Fusion, PRX Energy 3, (2024) 43002.

[11] Y. Song, X. Zou, X. Gong, A. Becoulet, R. Buttery, P. Bonoli, T. Hoang, R. Maingi, J. Qian, X. Zhong, A. Liu, Realization of thousand-second improved confinement plasma with Super I-mode in Tokamak EAST, Sci. Adv. 9, (2023) eabq5273.

[12] J. M. Gao, L.Z. Cai, X.L. Zou, T. Eich, J. Adamek, C.Z. Cao, Z.H. Huang, X.Q. Ji, M. Jiang, L. Liu, J. Lu, Type-I ELM power loads on the closed outer divertor targets in the HL-2A tokamak, Nucl. Fusion 61, (2021) 066024.

[13] S. Wang, J. Li, Y. Wang, X. Zhang, R. Wang, Y. Wang, and J. Cao, Thermal damage of tungsten-armored plasma-facing components under high heat flux loads, Sci. Rep. 10, (2020) 1359.

[14] M. Wirtz, J. Linke, T. Loewenhoff, G. Pintsuk, and I. Uytdenhouwen, Transient heat load challenges for plasma-facing materials during long-term operation, Nucl. Mater. Energy 12, (2017) 148.

[15] C. Ham, A. Kirk, S. Pamela, and H. Wilson, Filamentary plasma eruptions and their control on the route to fusion energy, Nat. Rev. Phys. 2, (2020) 159.

[16] G. Sinclair, J. K. Tripathi, P. K. Diwakar, and A. Hassanein, Melt layer erosion during ELM-like heat loading on molybdenum as an alternative plasma-facing material, Sci. Rep. 7, (2017) 12273.

[17] V. Sizyuk and A. Hassanein, New proposed ITER divertor design using carbon insert on tungsten to mitigate ELMs and secondary radiation effects on nearby components, Sci. Rep. 12, (2022) 4698.

[18] A. Hassanein, T. Sizyuk, V. Sizyuk, and G. Miloshevsky, Impact of various plasma instabilities on reliability and performance of tokamak fusion devices, Fusion Eng. Des. 85, (2010) 1331.

[19] M. Rieth, S.L. Dudarev, S.G. De Vicente, J. Aktaa, T. Ahlgren, S. Antusch, D.E.J. Armstrong, M. Balden, N. Baluc, M.F. Barthe, W.W. Basuki, Recent progress in research on tungsten materials for nuclear fusion applications in Europe, J. Nucl. Mater. 432, (2013) 482.

[20] M. S. Shaikh, H. A. Pathak, T. Oliver, and X. Wang, Structural finite element analysis of ITER In-wall shield, Fusion Eng. Des. 88, (2013) 2105.

[21] C. Li, D. Zhu, B. Wang, and J. Chen, Theoretical analysis on the damages for tungsten plasma facing surface under superposition of steady-state and transient heat loads, Fusion Eng. Des. 132, (2018) 99.

[22] M. Rieth, S.L. Dudarev, S.G. De Vicente, J. Aktaa, T. Ahlgren, S. Antusch, D.E.J. Armstrong, M. Balden, N. Baluc, M.F. Barthe, W.W. Basuki, Recent progress in research on tungsten materials for nuclear fusion applications in Europe, J. Nucl. Mater. 432, (2013) 482.

[23] M. Wirtz, J. Linke, G. Pintsuk, G. De Temmerman, and G. M. Wright, Thermal shock behaviour of tungsten after high flux H-plasma loading, J. Nucl. Mater. 443, (2013) 497.

[24] M. Wirtz, J. Linke, G. Pintsuk, J. Rapp, and G. M. Wright, Influence of high flux hydrogen-plasma exposure on the thermal shock induced crack formation in tungsten, J. Nucl. Mater. 420, (2012) 218.

[25] A. Huber et al., Combined impact of transient heat loads and steady-state plasma exposure on tungsten, Fusion Eng. Des. 98–99, (2015) 1328.

[26] A. Shokry, S. Gowid, H. Mulki, and G. Kharmanda, On the Prediction of the Flow Behavior of Metals and Alloys at a Wide Range of Temperatures and Strain Rates Using Johnson–Cook and Modified Johnson–Cook-Based Models: A Review, Materials. 16, (2023) 1574.

[27] Y. Bian, G. Jin, L. Wang, R. Xue, Z. Li, and X. Deng, Mechanical properties and JC constitutive modification of tungsten alloys under high strain rates and high/low temperatures, Mater. Today Commun. 41, (2024) 110542.

[28] C. Bermudo Gamboa, T. Andersson, D. Svensson, F. J. Trujillo Vilches, S. Martín-Béjar, and L. Sevilla Hurtado, Modeling of the fracture energy on the finite element simulation in Ti6Al4V alloy machining, Sci. Rep. 11, (2021) 18490.

[29] L. Chen, S. Jiang, S. Zhang, W. Li, S. Hao, C. Li, H. Shi, and X. Li, Computational study of tungsten cracking propagation under ELM-like high heat flux conditions, J. Nucl. Mater. 605, (2025) 155567.

[30] M. Sun, W. Cao, D. Hu, N. Zhang, and R. Chi, Effect of Cover Plate on the Ballistic Performance of Ceramic Armor, Materials 14, (2021).

[31] M. Li, A Fracture Mechanics Study of Tungsten Failure under High Heat Flux Loads, (2015).

[32] J. Lee, Analysis of Multi-Layered Materials Under High Velocity Impact Using CTH, (2008) 198.

[33] S. H. Chang, C. I. Lee, and S. Jeon, Measurement of rock fracture toughness under modes I and II and mixed-mode conditions by using disc-type specimens, Eng. Geol. 66, (2002) 79.